

Design, Analysis, Prototyping and Testing of Aerofoils for High-Lift at Low Reynolds Number



Pavan Rayar

Abstract Increased payloads, reduced aircraft noise, shortened takeoff and landing distances and lowered stall speeds can all be achieved from the direct effects of improved high-lift aerofoil aerodynamics. It is, therefore, not surprising that the high-lift aerofoil design has been and will remain a topic of interest. Along with the interest, the opportunity is to make it more cost-effective. One possible way to achieve the objective is to build a cheaper yet simpler high-lift system. This presents a challenge to the high-lift aerodynamicist: to design a less complex flap that maintains high-lift and meanwhile lowers the flow separation. Furthermore, by designing the high-lift system to achieve longer attachment of flow onto the flap, aircraft noise will be reduced. This research article presents the design, analysis and prototyping and testing of aerofoil which was carried out after performing a literature survey on the performance of many aerofoils at low Reynolds number. This research was achieved using Vortex generators for high lifts. The prototype was tested in the wind tunnel.

Keywords Lift to drag ratio · CFD · Wind tunnel

1 Introduction

The aerofoil is the wing, rotor blade or sail shape as seen in cross-section. Such an aerodynamic body is meant to produce an aerodynamic force if it is moved on a fluid. The component which is perpendicular to the direction of motion is called the lift and the component parallel to the direction of motion is called the drag. Subsonic flight aerofoils have a characteristic shape with a rounded leading edge, followed by a sharp trailing edge, often with asymmetric camber.

Though the earliest serious work on the development of aerofoil sections began in the late 1800s, the development of the modern aerofoils for wind turbines began

P. Rayar (✉)

Department of Production Engineering, Dwarkadas J. Sanghvi College of Engineering, Mumbai, India

e-mail: pavan.rayar@djsce.ac.in

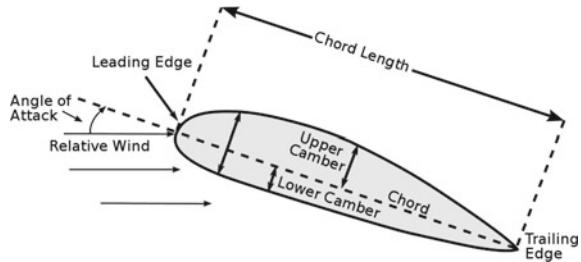
© Springer Nature Singapore Pte Ltd. 2020

H. Vasudevan et al. (eds.), *Proceedings of International Conference on Intelligent*

Manufacturing and Automation, Lecture Notes in Mechanical Engineering,

https://doi.org/10.1007/978-981-15-4485-9_70

Fig. 1 The nomenclature of aerofoil



in the 1980s. The requirements for such aerofoil differ from standard aviation aerofoils, because of structural reasons and extensive aerodynamic off-design operation conditions. During high wind speeds, wind turbine aerofoils usually operate under fully separated flow when the stall is used for power regulation (Fig. 1).

For simplicity, aerodynamicists follow a convention that allows for the summation of all the very complex aerofoil components in one quantity, the lift coefficient (CL). It determines how well the aerofoil works as a source of lifts. In addition to the lift, there is always a force that directly opposes the wing's movement through air, and is called drag. This component of force is conveniently described by the coefficient of drag (CD). Drag Force is also influenced by the shape of aerofoil and angle of attack

$$FL = \frac{1}{2} \rho v^2 CL A \quad (1)$$

$$F = \frac{1}{2} \rho v^2 C D A \quad (2)$$

Here,

FL = Lift Force, FD = Lift Force, ρ = Density of fluid, v = velocity of free stream, CL = Lift Coefficient, A = Wing Area.

2 Literature Survey

Miley [1] cataloged the results of test conducted on NACA 66(2)-415 aerofoil. For high-lift at low Reynolds number. This test was conducted in 1982 for Rockwell international corporation energy system groups which were a part of the United States Department of energy for the wind energy department under the federal wind energy program. The aerofoil was tested in a close circuit wind tunnel at 40 m/s and Reynolds number of about 7×10^5 . An investigation was conducted in the Langley low-turbulence pressure tunnel to evaluate the two-dimensional low-speed aerodynamic characteristics of a 17% thick aerofoil designed for general aviation applications. The findings are compared to the standard older NACA 65 series aerofoil section. A comparison of experimental data and projections is also provided, based on a

theoretical framework for measuring the viscous flow about the aerofoil range from -10° to 24° . Reynolds numbers, based on the aerofoil chord, were varied from about 2.0×10^6 to 20.0×10^6 . The results of the investigation indicate that maximum section lift coefficients increased rapidly at Reynolds numbers from about 2.0×10^6 to 6.0×10^6 attained values greater than 2.0 for the plain aerofoil and that for an aerofoil with 20% chord split greater than 3.0. Stall characteristics were seen generally gradual and of the trailing edge type either with or without the split-flap [2]. The NACA 4 and 5 digit sections investigated consisted of the NACA 0012, and the NACA 44 and 230 series sections of 12 and 15% conditions and also included the determination of the effectiveness of the different aerofoils at various Reynolds number when equipped with split flaps [3]. Roughness on the leading edge materially reduced the effect of Reynolds number on maximum lift coefficient, but Mach number effects [4]. The test results revealed considerable maximum lift effects on the three-element landing configuration for Reynolds number variations and significant Mach number effects on the four-element aerofoil [14]. The research paper [18] describes a separate eddy simulation (DES) for a single flow over aerofoil of NACA 00012. Differences were plotted between 2 and 3 dimensional contours, as well as contours of vorticity and entropy. As compared to 2D and 3D URANS, the 2D DES showed an increase in lift and drag predictions. The 3D URANS, DES lift and drag, however, are similar to the experimental results.

3 Statement of Problem and Methodology

It is recommended that the Cambered aerofoil Shape and certain other devices be used to improve lift at the same working conditions by reviewing all of the above Papers and carrying out research work carried out to date on the design of a high-lift aerofoil giving more lift at low Reynolds number. The easiest and best way to improve lift at the same working condition is to have Vortex generators working on the principle of delayed boundary layer separation.

Methodology applied to address the statement of the problem was as follows:

1. To design the best suitable aerofoil for high-lift at lower speeds the NACA 2415 aerofoil will be analyzed first at various angle of attacks to study its performance and draw conclusions regarding the same, thus bettering our understanding of the phenomenon of achieving higher lifts at low Reynolds number or low speeds.
2. To find the separation and reattachment points onto the aerofoil the Ansys 14.0 will be used.
3. The different types of Vortex generators are added onto the upper surface of aerofoil and analyzed for the same speed at various angle of attacks.
4. After getting satisfactory results in the analysis the same model will be 3D printed or Prototyped to validate the results obtained in analysis with the experiments value being conducted on Wind Tunnel.

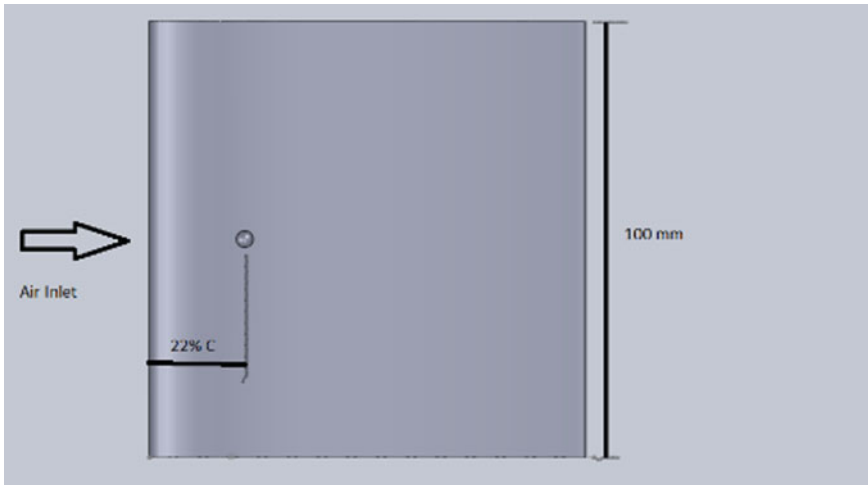


Fig. 2 Top view of NACA 2415 aerofoil with a Single Dimple at a distance of 22% of chord from leading edge

4 Design and Analysis

The aerofoil selected is NACA 2415, which is a low Reynolds number and is perfectly suited for the available wind tunnel set-up. The NACA 2415 aerofoil has a maximum thickness of 15%, Camber 2% located 40% back from the leading edge. Using mathematical relationships, (m , p and t) these values can be used to measure the coordinates for a whole aerofoil and then the same thing is CAD modelled in SolidWorks 10.0.

The CAD model of NACA 2415 is analyzed on Ansys to find the separation point then the aerofoil is modified by adding the Vortex generators on the above side (called DIMPLE MODEL) and again analyzed and compared with the earlier model (Figs. 2 and 3).

This section reflects the results obtained from the numerical evaluation on both the Plain and Dimpled Models for Velocity, Pressure, coefficient of lift and coefficient of drag Figs. 4, 5, 6, 7, 8, 9, 10, 11, 12, 13, 14, 15, 16, 17, 18, 19, 20, 21, 22, 23, 24 and 25.

5 Prototyping and Experimentation

Both the models (plain model and Dimpled model) were prototyped on a 3D printer with SLA technology (Stereolithography) and have been analyzed for C_l and C_d on Wind Tunnel. The following observations were made for both the models (Fig. 26).

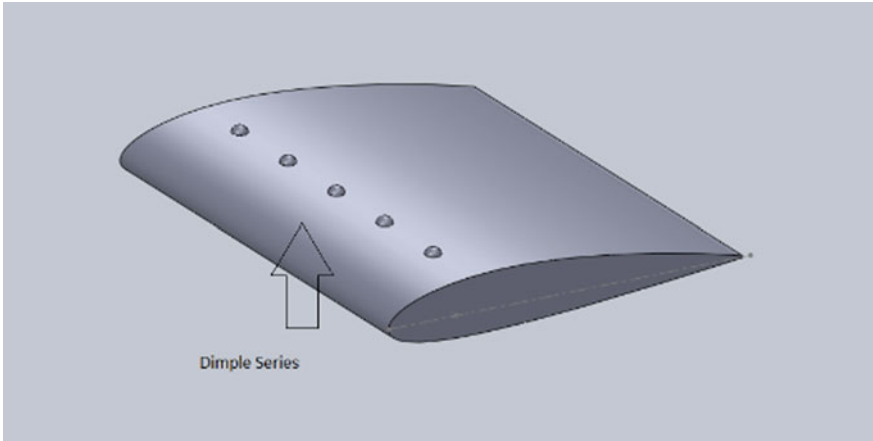


Fig. 3 Isometric view of NACA 2415 aerofoil with Dimple series

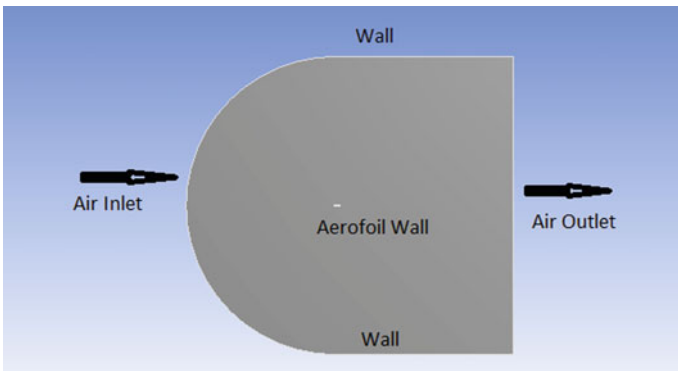


Fig. 4 The Ansys environment (boundary conditions)

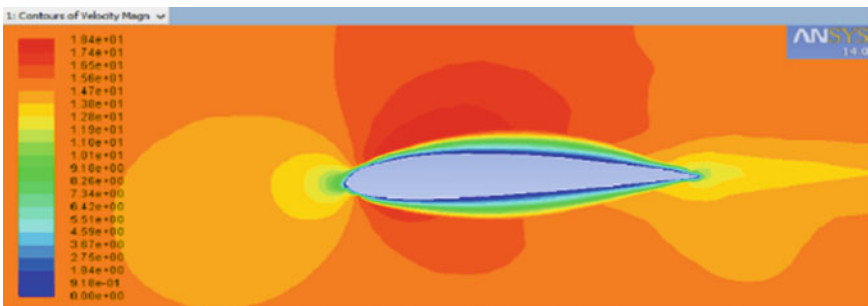


Fig. 5 Velocity contour for plain model at 0°

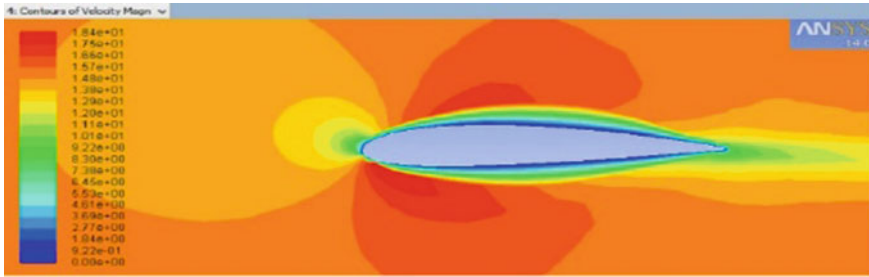


Fig. 6 Velocity contour for plain model at -5°

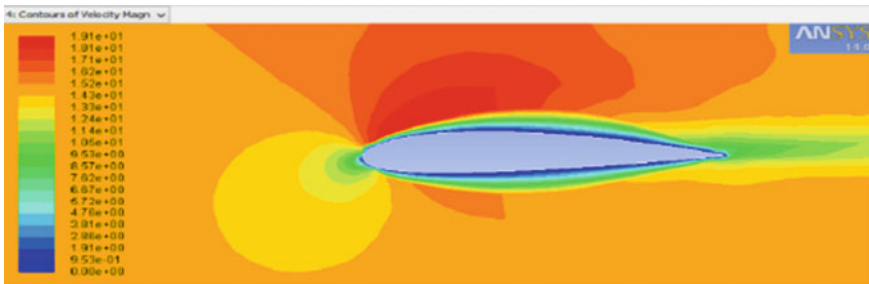


Fig. 7 Velocity contour for plain model at 5°

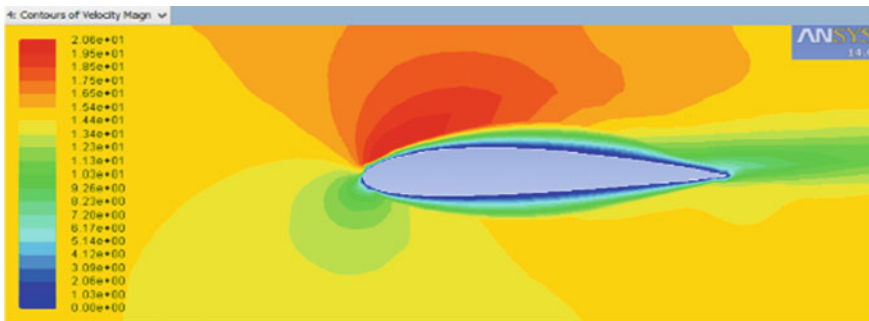


Fig. 8 Velocity contour for plain model at 10°

Observations were made for both Plain and Dimpled model and results were tabulated which intern helped to depict the results in the form of graphs in the next section.

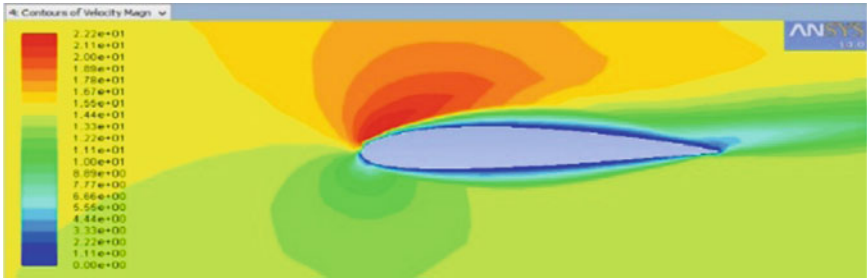


Fig. 9 Velocity contour for plain model at 15°

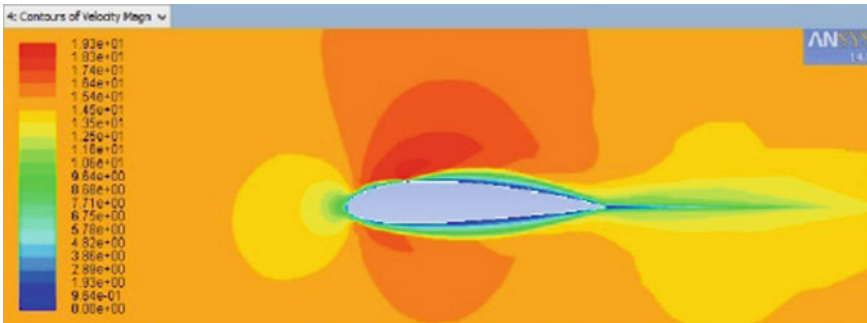


Fig. 10 Velocity contour for Dimpled model at 0°

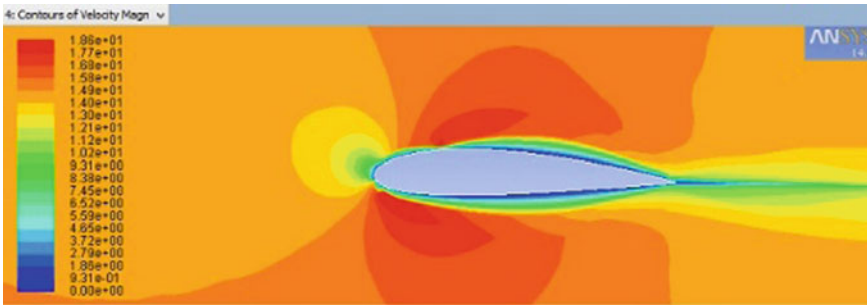


Fig. 11 Velocity contour for Dimpled model at -5°

6 Results

The following graphs were plotted for coefficient of lift and coefficient of drag for both the models against different angle of attack (AOA) and compared to find which model worked more efficiently as given under.

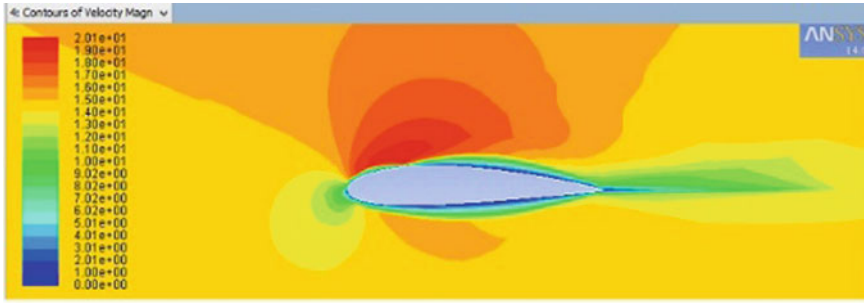


Fig. 12 Velocity contour for Dimpled model at 5°

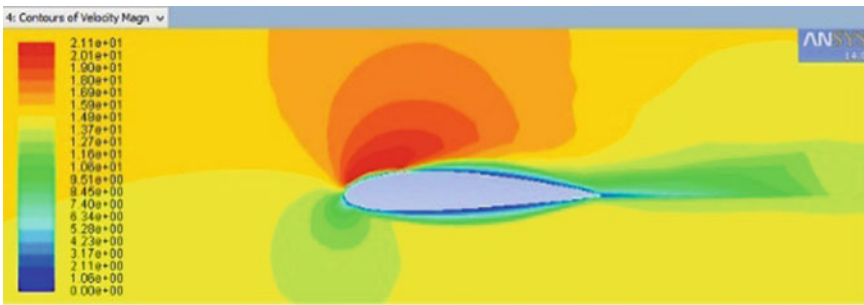


Fig. 13 Velocity contour for Dimpled model at 10°

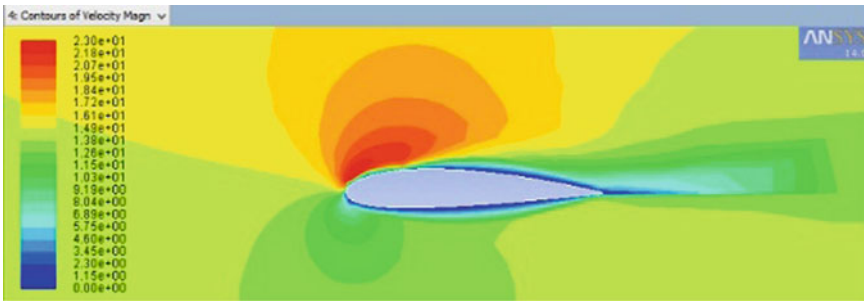


Fig. 14 Velocity contour for Dimpled model at 15°

Figure 27 shows the variations of C_l against different angle of attack for Dimpled model (Fig. 28).

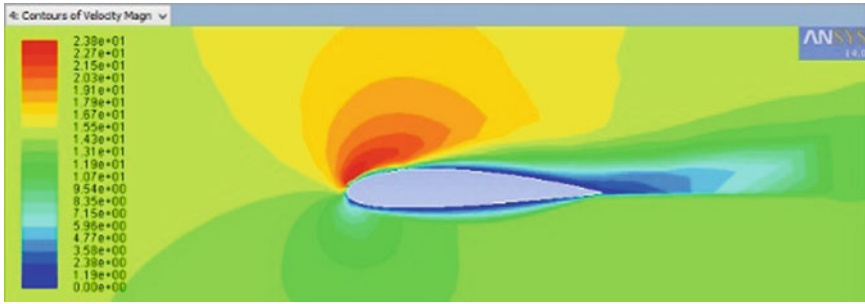


Fig. 15 Velocity contour for Dimpled model at 18°

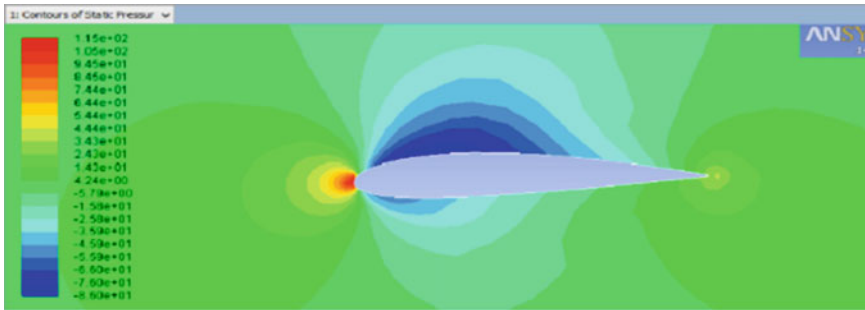


Fig. 16 Pressure contour for plain model at 0°

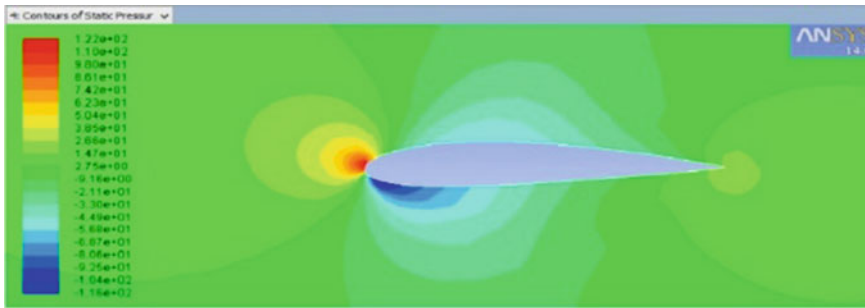


Fig. 17 Pressure contour for plain model at -5°

7 Conclusion and Future Scope

By the comparison held for both the Plain and Dimpled models for NACA 2415 under the same working conditions, it was observed that the Dimpled model has performed well and has achieved a 11% high coefficient of lift and 9% less coefficient of drag as compared to the plain model.

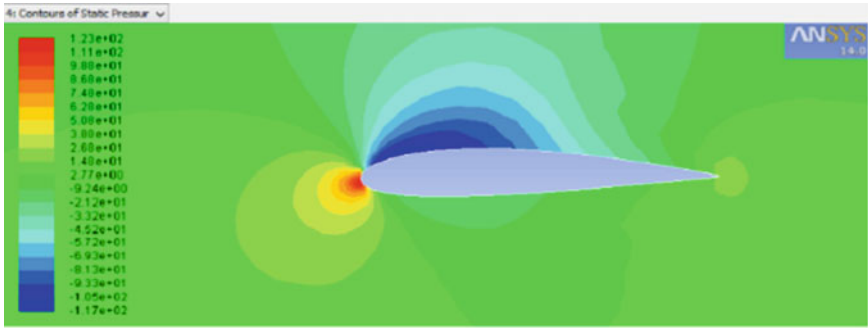


Fig. 18 Pressure contour for plain model at 5°

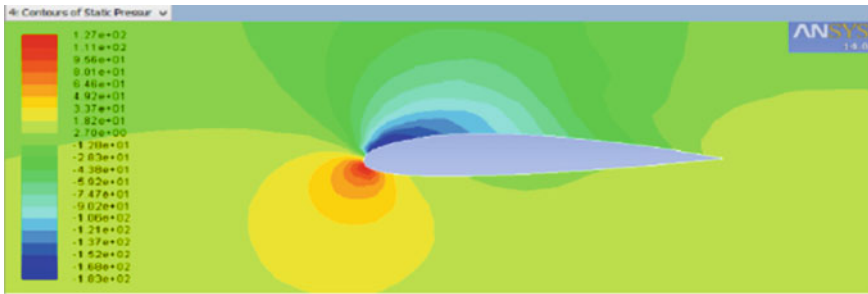


Fig. 19 Pressure contour for plain model at 10°

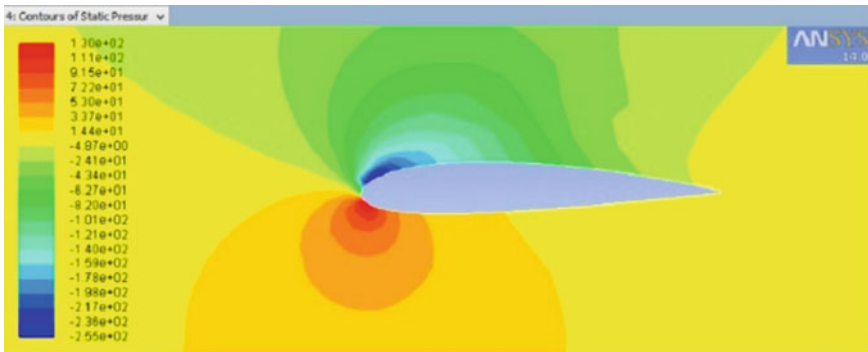


Fig. 20 Pressure contour for plain model at 15°

The experimental values were depicted in Graphical form. The Dimpled model performed well in the same environment given to the plain model by producing 11% more coefficient of lift compared to plain model and 09% less coefficient of drag compared to plain model. From 4° to 17° the CL increased continuously and the ratio

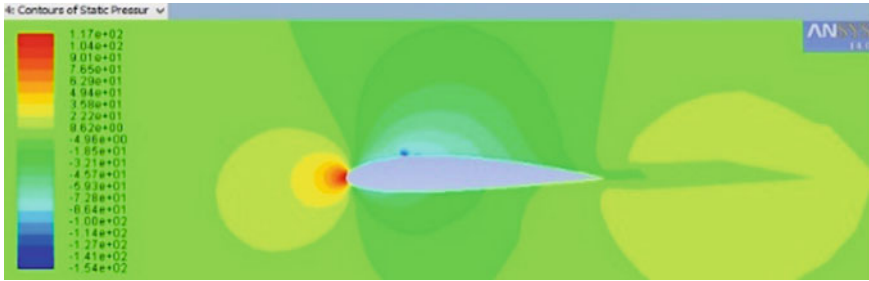


Fig. 21 Pressure contour for Dimpled model at 0°

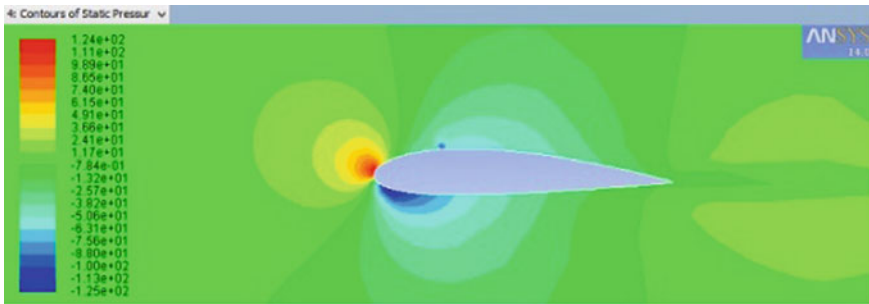


Fig. 22 Pressure contour for Dimpled model at -5°

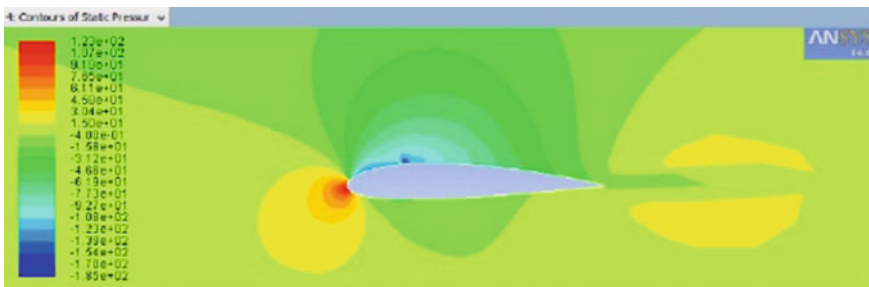


Fig. 23 Pressure contour for Dimpled model at 5°

of L/D was over 1. Within this range, the aerofoil is utilized efficiently. The research showed that the Vortex generators can be used in different ways with different shapes and sizes on the upper surface for delayed separation. The research can be further taken ahead with Positioning of the Vortex Generators with a combination of other moving elements.

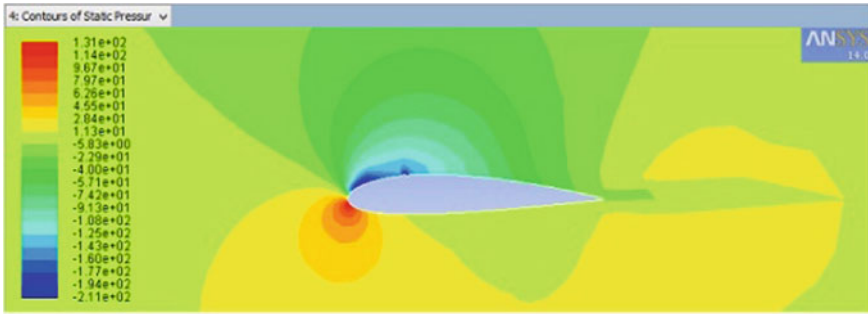


Fig. 24 Pressure contour for Dimpled model at 10°

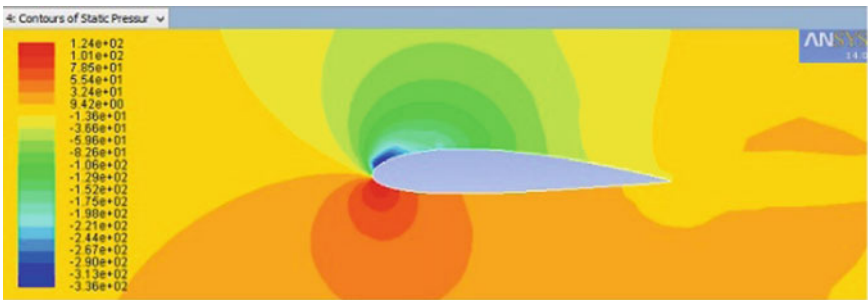


Fig. 25 Pressure contour for Dimpled model at 18°



Fig. 26 The plain model of the aerofoil (by Wirecut M/C)

Fig. 27 Coefficient of lift and coefficient of drag versus AOA for both models

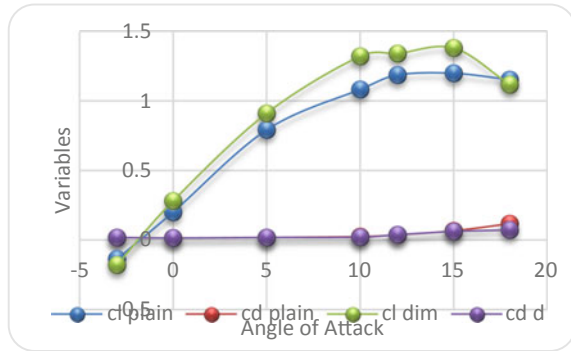
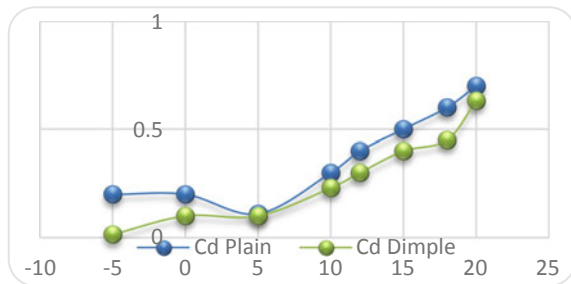


Fig. 28 Comparison of coefficient of drag for both models versus angle of attack



Bibliography

1. Selig MS, Guglielmo JJ (1997) High-lift low Reynolds number airfoil design. *J Aircr* 34(1):72–79
2. Merabet A, Necib B (2003) Characterisation of wings with NACA 0012 airfoils. *Rev. énergies Renouvelables* 2:131–137
3. Kunz PJ, Kroo I (2001) Analysis and design of aerofoil’s for use at ultra low Reynolds numbers. *Prog Astronaut Aeronaut* 195:35–60 (Mueller TJ (ed))
4. Rumsey CL, Gatski TB, Ying SX, Bertelrud A (1998) Prediction of high-lift flows using turbulent closure models. *AIAA J* 36:765–774
5. McCullough ME, Kilpatrick SD, Emmons RA, Larson DB (2004) Is gratitude a moral affect? *Psychol Bull* 127:249–266
6. Carmichael BH (1981) Low Reynolds number aerofoil survey, vol 1. NASA contractor report 165803, Nov 1981
7. Guilmineau E, Piquet J, Queutey P (1997) Two-dimensional turbulent viscous flow. *Comput Fluids* 26(2):135–162
8. Loftin LK, Poteat MI. Aerodynamic characteristics of several NACA airfoil sections at seven Reynolds numbers from 0.7×10^6 (exp 6) to 9.0×10^6 (exp 6)
9. Srivastav D (2012) Flow control over airfoils using different shaped dimples, vol 33, no. Fdtt, pp 92–97 (2012)
10. Anderson JD Jr (2001) *Fundamentals of aerodynamics*. McGraw Hill
11. Sathaye SS (2004) Lift distributions on low aspect ratio wings at low Reynolds numbers, May
12. Mirzaei M, Ardekani MA, Doostlab M (2009) Numerical and experimental study of flow field characteristics of an iced airfoil. *Aerosp Sci Technol* 13:267–276

13. Emami MR (2007) Aerodynamics forces on an aerofoil. Presented at Aerospace Undergraduate Laboratories-University of Toronto in 2007, for research on lift on aerofoil and forces acting on aerofoil
14. You D, Moin P (2008) Active control of flow separation over an airfoil using synthetic jets in 2008. *J Fluids Struct* 24:1349–1350
15. Hoerner SF (1965) Fluid dynamic drag. In: *Hoerner fluid dynamics*, Brick Town, NJ, pp 7.16–7.21
16. Gad-el-Hak M (2001) Micro-air-vehicles: can they be controlled better. *J Aircr* 38(3):419–429
17. Schlichting H (1979) *Aerodynamics of the airplane*. Mc-Graw-Hill International Book Company, pp 143–161
18. Torres G, Mueller TJ (2001) Aerodynamic characteristics of low aspect ratio wings at low Reynolds number. *Prog Astronaut Aeronaut* 195:115–141 (Mueller TJ (ed))
19. Pelletier A, Mueller TJ (2000) Low Reynolds number aerodynamics of low-aspect-ratio, thin/flat/cambered-plate wings. *J Aircr* 37(5):825–832
20. Spalart PR, Allamaras SR (1992) A one-equation turbulence model for aerodynamic flow. *AIAA Pap* 92:0439
21. OpenFOAM, the Open Source CFD Toolbox user guide, version 1.4.1, 1 Aug 2007, copyright 2000, 2001, 2002, 2003, 2004, 2005, 2006, 2007 OpenCFD limited
22. Ghia U, Ghia KN, Shin CT (1982) High-Re solutions for incompressible flows using the Navier-Stokes equations and a multigrid method. *J Comput Phys* 48:387–411 (in the Langley 8-foot transonic pressure tunnel, NASA TM 81927)
23. Mangler (1939) Induced drag analysis in small aspect ratios. *Yearbook D.Lufo*, p.I 139